AIDIC *Conference Series*, Vol. 9, 2009
Editor Sauro Pierucci
DOI: 10.3303/ACOS0909037

ISBN 978-88-95608-10-5 ISSN 2036-5969

PARTICLE DISTRIBUTION IN AN UNBAFFLED STIRRED VESSEL BY A NOVEL LASER SHEET IMAGE ANALYSIS TECHNIQUE

A.Tamburini, A. Cipollina, G. Micale, A. Brucato

Dipartimento di Ingegneria Chimica dei Processi e dei Materiali, Università di Palermo, Italy

The availability of experimental information on solid distribution inside stirred tanks is a topic of great importance in several industrial applications. The measurement of solid particle distribution in turbulent multiphase flow is not simple and the development of suitable measurement techniques is still in progress. In this work a novel non-invasive technique for measuring particle concentration fields in solid-liquid systems is presented and employed. The technique makes use of a laser sheet, a high sensitivity digital camera for image acquisition and a Matlab procedure for post-processing the acquired images.
Experimental data are here obtained for the case of an unbaffled stirred tank provided with cover. Stable toroidal attractors for particles are observed under given circumstances. Their existence, consistency and extension dependence on particle inertia properties and impeller angular velocity is investigated and discussed.

1. INTRODUCTION

Suspensions of solid particles in liquids are largely employed in a number of applications. Such operation is commonly carried out in tanks stirred by suitable mechanical agitators. Most industrial stirred vessels are equipped with baffles, which ensure better axial circulation and mixing with respect to the case without baffles. However, there are many applications (Assirelli et al., 2008; Pacek et al., 2001), in which the use of baffles could generate some specific drawbacks. For example, in food and pharmaceutical industries it is matter of primary importance to keep the reactor as clean as possible. In crystallization processes (Hekmat et al., 2007) and biological application (Aloi and Cherry, 1996) where it is necessary to avoid any damage on growing particles or on cells culture, respectively. In precipitation processes baffles could suffer from incrustation problems (Rousseaux et al., 2001). Moreover unbaffled vessels are preferentially adopted for the case of laminar mixing: they are preferred for this flow regime because in baffled systems some dead regions may exist in front of baffles.

In order to study the suspension of solid particles in stirred tank, a novel technique has been purposely developed, taking into account all the main, positive and negative, features of the measurement techniques available in literature for stirred tanks. Today, in scientific literature, two macro-categories of methods for the solid particle distribution assessment inside a stirred vessel exist: the *invasive techniques* and the *non-invasive techniques*.

The sampling method and the measurement probes techniques belong to the first class. The first one provides for taking samples from suspensions in many different points of the stirred tank thus successively measuring their solid concentration value (Barresi and Baldi, 1987). Such a methodology strongly suffers of a poor reproducibility of the results because they are highly dependent on both the forms and the entrance of the used sampling probes (Godfrey and Zhu, 1994).

The measurement probes techniques can be classified in three different sub-categories on the basis of the specific variable they measure: impedance, optic and acoustic techniques.

Impedance techniques (McKee et al., 1995; Brunazzi et al., 2004; Spidla et al., 2005) provide for assessing the impedance (or only the capacity or only the conductivity) between two electrodes present inside the probe: the

Please cite this article as: Tamburini A., Cipollina A., Micale G. and Brucato A., (2009), Particle distribution in an unbaffled stirred vessel by a novel laser sheet image analysis technique, AIDIC Conference Series, 09, 319-328 DOI: 10.3303/ACOS0909037

value resulting depends on the local solid particle quantity met by the electric flow lines, therefore it allows the local solid concentration calculation.
Optical techniques provide for the employment of photoelectric capillaries (Lu et al., 1993; Thompson and Worden, 1997) or endoscopies (Angst and Kraume, 2006) or turbidimetric analysis (Sessiecq et al., 1999), all instruments and equipments are able to transform light attenuation measurement in an indirect local particle concentration assessment.
The last category of measurement probe techniques make use of acoustic spectroscopy (Alba et al., 1999; Bamberger and Greenwood, 2004). This method can be employed both for dilute and very concentrated solid-liquid systems. It is practically based on the measurement of the attenuation that an acoustic wave undergoes while crossing the suspension. The acoustic method is quite similar to the optical one but an acoustic wave can pass through very dense suspensions, an impossible objective for a light ray.
Naturally, all the intrusive techniques have the negative feature of requiring the probe presence (for sampling or measurement) inside the stirred tank: this presence could change the system flow field and consequently alter the deduced results. Moreover, most of these methods allows only local assessments, thus requiring too much measurements and as much interpolations among the obtained local data.
The main non-intrusive techniques known in literature are: the light attenuation, the radiative and the tomographic techniques.
The first ones (Bohnet et al., 1980; Magelli et al., 1990) provide for the presence of an emitter and a photo-diode both placed outside the vessel, which measure the attenuation that a ray light undergoes while it is crossing the same vessel: a ray light is more adsorbed when it passes through a suspension than a poor liquid. The same theoretical principle lies behind the radiative techniques (Fournier et al., 1993), but instead of a ray light, they employ X-rays, or χ-rays, or neutrons beams. The results obtainable by these two methods are very reliable, but, they concern only the mean solid concentration along the line covered by the beam. In addition, a lot of experiments are necessary to avoid the use of too much interpolations in getting a solid concentration distribution map.
The tomographic techniques are advantageous since they allow to get 2D distribution maps of solid concentration in stirred tanks. There are two different types of tomographic methods: the Electrical Resistance Tomography (*ERT*) and the Positron Emission Particle Tracking (*PEPT*).
The *ERT* (McKee et al., 1995; Wang et al., 2000) makes use of a series of electrodes, coupled two by two (anode and cathode) and disposed around the vessel to investigate. It measures the electrical signals, taken from all possible views of sensing electrodes surrounding the tank, but the presence of electrical noise may alter the reliability and the exactness of results.
The *PEPT* (Parker et al., 1993; Fangary et al., 2002; Barigou et al., 2003; Guida et al., 2009) involves the use of a labelled tracer particle, a positron camera and a location algorithm for computing the tracer location. The tracer particle is labelled with a positron-emitting isotope. A positron emitted by the particle tracer rapidly annihilates with an electron emitting a pair of almost collinear 511 keV γ-quanta in opposite directions, 180 degrees apart. These two γ-rays hit two position-sensitive detectors, thus allowing to track the radioactive particle in 3D space and time. The result of such an experiment is a distribution map of particle position probability, that is an indirect measurement of a concentration distribution map. This technique is also able to characterize suspensions with high concentration, but it is too expensive and it is not able to deal with systems with an agitation speed lower than the complete suspension velocity. In fact, under such conditions, a sediment lies on the tank bottom and the tracer particle could be trapped there without provide any useful information.
Considering the limits and disadvantages concerning all the techniques described so far, the idea of proposing a new measurement technique arises. Obviously, it would be innovative, non-invasive and able to produce reliable 2D solid distribution maps at acceptable costs and in reasonable times. This new technique was namely *Laser Sheet Image Analysis (LSIA)* and it will be described in detail in the relevant paragraph.
For the purpose of the present work the *LSIA* technique has been applied to the case of a solid-liquid suspension in a standard geometry unbaffled stirred tank. The existence conditions of two stable toroidal zones, resulting in attractors for non-Brownian particles, heavier than the fluid, is investigated under turbulent conditions. Naturally, the vortex formation under this flow regime is avoided by both covering and degassing the vessel, thus consequently eliminating the dependence of the Power number on the Froude number.

2. EXPERIMENTAL APPARATUS AND *LSIA* FUNDAMENTALS

The experimental system consists of three main parts: the investigated vessel, the degassing unit and the *LSIA* apparatus.

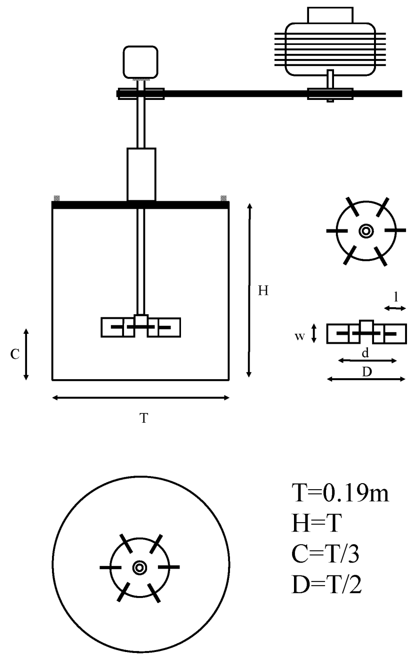

Figure 1: The investigated vessel

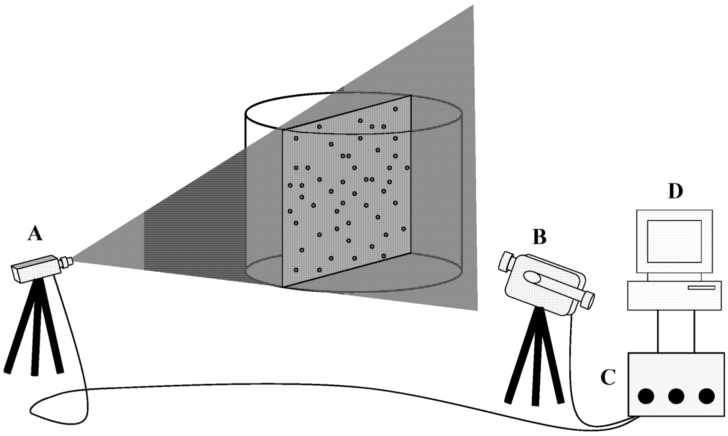

Figure 2: LSIA apparatus: A) pulsed laser; B) videocamera; C) control-acquisition unit; D) personal computer

The vessel is a cylindrical, flat-bottomed, standard geometry unbaffled tank with a diameter T=0.19m, equipped with a six-bladed Rushton turbine (Fig.1). To solve any optical distortion problems, the stirred vessel was inserted inside a bigger tank with a rectangular plant, accurately placed with the faces perpendicular to the laser and the videocamera action directions. The impeller is moved by an electric synchronous engine *MAVILOR*, *MSS-8 type*, supplied by continuous current by an external feeder. This feeder is equipped with a feedback (PID) *INFRANOR* controller able to ensure the angular velocity set point.

A fundamental task in conducting experiments is to avoid the presence of air or simply air bubbles within the stirred vessel. Air could generate vortex under turbulent regime and bubbles could be mistaken for solid particles during the acquisition procedure, thus altering results reliability. So the investigated vessel is covered by a holed metal plate and contemporaneously connected with a purposely developed degassing system.

The *LSIA* apparatus is depicted in Fig.2: it consists of the illumination system, the acquisition system, the synchronization system and a PC provided with the relevant software. The illumination equipment is a double cavity ND:YAG pulsed laser of the *NEW WAVE RESEARCH*, *Solo III 15Hz* model. It is a state solid laser emitting a infrared radiation which is transformed in a luminous radiation by a suitable frequency doubler. Finally, such a laser is equipped with a semi-cylindrical optics *Dantec* 80x11 able to transform the ray emitted in a light sheet in order to light up the section to investigate The acquisition system is a *Dantec 80C60 Hisense PIV* characterized by a 1280x1240 pixels CCD. It has a very high sensibility to light and it is equipped by a pass-band filter of the *Edmund Scientific* centred on the wave length of 532 nm in order to limit the luminous noise due to other external light sources. Obviously, the videocamera-vessel relative position is to be accurately chosen in order to avoid any parallax error. The synchronization of the emitting-acquisition times of laser and videocamera are guaranteed by an acquisition-control unit with a *DANTEC* processor, *Flow Map 1500* model. This processor is connected via Ethernet peer to peer connection to a PC. The software utilized are the *Flow*

Manager ver.3.7 and the *Matlab*. The laser light sheet frequency was not be equal or a multiple of the rotating frequency of the impeller in order to acquire images at various impeller blade positions.

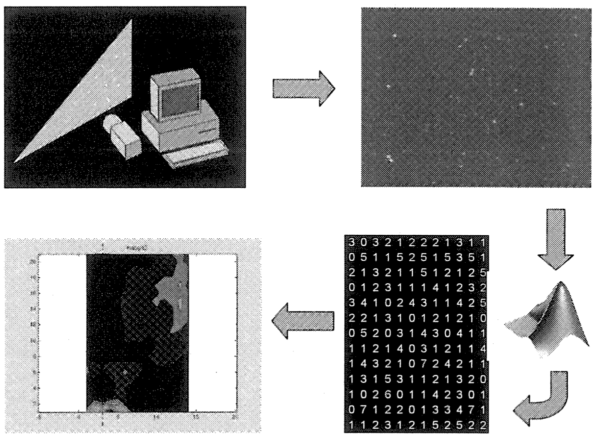

Figure 3: LSIA main phases

The novel *Laser Sheet Image Analysis* technique is based on the probabilistic elaboration of acquired images (Fig.3). A horizontal or vertical section of the investigated vessel is illuminated by a pulsed laser sheet; in this work only half diametrical vertical section is investigated. Solid particles are stochastically intercepted by the laser blade and appear as bright little points, whose spatial distribution is captured by the videocamera, purposely placed perpendicularly to the illuminated plane. Both the laser and the camera have a fixed position in space. By suitably synchronizing the pulsed laser and the videocamera, it is possible to obtain an image. It is a grey-scale background image with some white peaks that correspond to the presence of particles. The images obtained in this way are elaborated in order to identify the particles and their position, accurately filtering those spurious white peaks that are not linked to the presence of particles. Then, by acquiring a high number of images (i.e. 2000) and by summing all their relevant position matrixes, it is possible to get a 2D particle presence probability ($counts_{r,z}$) distribution map. This sum-position matrix is compressed about 5 times ($\Delta r = \Delta z \approx 5$ pixels) in order to average the results and consequently reduce the data probabilistic scattering. Such a map, multiplied by a α constant (see below, par.2.1), corresponds to a solid phase concentration $C_{r,z}$ distribution map on the same vessel section.
All these elaborations are carried out by means of specific functions of the *Matlab image tool-kit*. All the experiments were performed by filling the tank with deionised water and particles with a concentration of 0.2 g/l. Glass ballottini (density of about 2500 kg/m^3) or white corundum particles (density of about 4000 kg/m^3) of different size (i.e 125-150 μm, 212-250 μm, 250-300 μm, 425-500 μm) were utilized in the experiments. In addition, four different angular velocities (i.e. 300 RPM, 400 RPM, 500 RPM, 600 RPM) were investigated for each case.

2.1 Shifting from a probability distribution map to a normalized concentration map

Each coefficient of the compressed sum-position matrix (that is a number of $counts_{r,z}$) refers to a little area of the illuminated plane (whose size are clearly Δr and Δz) and it represents the probability of finding a particle in that area. Because of the axial symmetry of the unbaffled vessel, there is the same probability in the volume generated by the rotation of the considered area. The α constant allows to shift from this local probability to the local concentration value $C_{r,z}$ which is the concentration value relevant to the former rotational volume. In formula:

$$C_{r,z} = counts_{r,z} \cdot \alpha \tag{1}$$

Therefore, the relevant local mass value $M_{r,z}$ can be estimated by multiplying the local concentration by the relevant rotational volume:

$$M_{r,z} = counts_{r,z} \cdot \alpha \cdot 2\pi r(\Delta r \cdot \Delta z) \quad \textbf{(2)}$$

The sum of all the local mass values results in the total mass value:

$$M_{TOT} \cong \sum_{r=1}^{T/2} \sum_{z=1}^{H} 2\pi r \cdot \Delta r \cdot \Delta z \cdot counts_{r,z} \cdot \alpha \quad \textbf{(3)}$$

In this way it is possible to estimate α since the total mass loaded in the tank is a known value:

$$\alpha = \frac{M_{TOT}}{2\pi \cdot \Delta r \cdot \Delta z \cdot \sum_{r=1}^{T/2} \sum_{z=1}^{H} r \cdot counts_{r,z}} \quad \textbf{(4)}$$

However, it is more interesting to obtain final maps where the local concentration is normalized as regards to the mean concentration inside the vessel C_m. Therefore inside the Matlab procedure it is used another constant, named K which is equal to the ratio of α to the mean concentration C_m.

$$\frac{C_{r,z}}{C_m} = \frac{counts_{r,z} \cdot \alpha}{\frac{M_{TOT}}{\pi R^2 H}} = counts_{r,z} \cdot K \quad \textbf{(5)}$$

The equation for the computation of the constant K is obtained by dividing α by the mean concentration.

$$K = \frac{\alpha}{\frac{M_{TOT}}{\pi R^2 H}} = \frac{R^2 H}{2 \cdot \Delta r \cdot \Delta z \cdot \sum_{r=1}^{T/2} \sum_{z=1}^{H} r \cdot counts_{r,z}} \quad \textbf{(6)}$$

Summarizing, it is possible to directly transform the probability map into a normalized concentration map simply multiplying the compressed sum-position matrix by this K value.

3. RESULTS AND DISCUSSION

Starting to operate from still conditions, all the particles begin to move from the bottom until they form the first torus (the *lower torus*) just below the impeller. Increasing the impeller rotational velocity, some particles run away from the lower torus to constitute the *upper torus* in the upper part of the vessel. Increasing further the agitation velocity, the number of particles moving from the lower torus towards the upper torus increases gradually. Therefore, at high impeller speeds particles prefer the upper torus more than the lower one. This evolution is well captured by the *LSIA* technique and it is visible for 425-500 microns glass ballottini in Fig.4: at 300RPM particles are all over the bottom, some as sediment and some circulating within the lower torus, at 400RPM many of them move towards the upper part of the vessel and form the second upper torus, at 500RPM and finally at 600RPM the amount of particles shifting from the lower torus to the upper one increases with the angular velocity. In addition, at 600RPM all the particles are suspended and no sediments are present. At velocities much higher than 600RPM, i.e. about 800RPM for the present case (glass ballottini of 425-500 microns), all the particles leave the lower torus transferring themselves in the upper one. These very high velocities were not investigated since the seal between the shaft and the upper part of the cover becomes less effective and some air bubbles enter inside the vessel compromising the experiments. However, at these high velocities, all the experiments performed showed the existence of the upper torus only. It is worth noting that, negligible concentration of particles are present in other vessel zones at any agitation speed, because almost all particles are essentially attracted by the two tori.

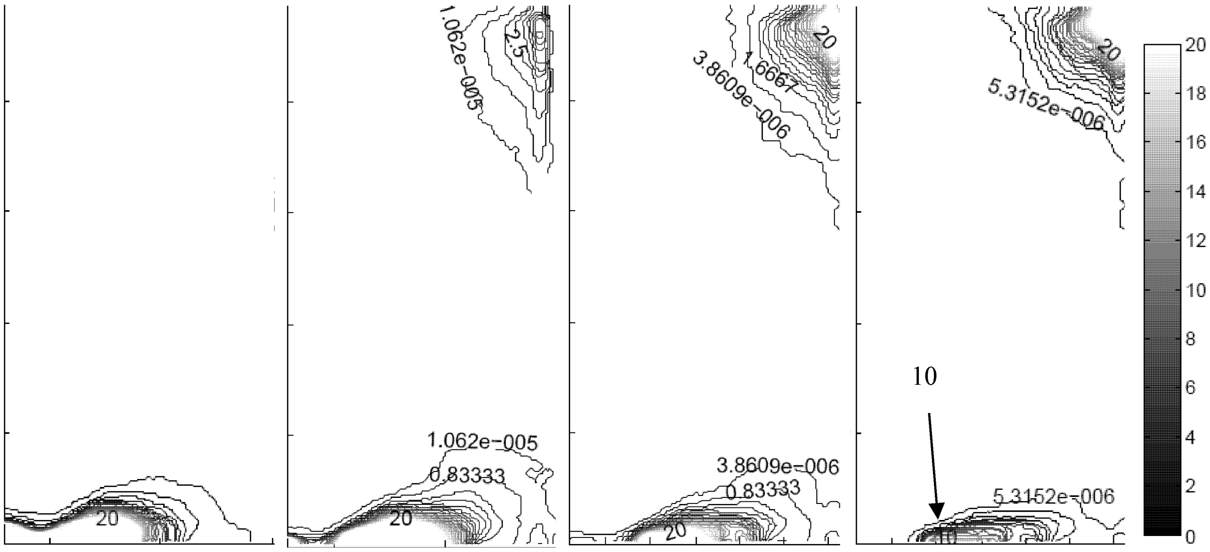

Figure 4: Contour plots of glass ballottini of 425-500 μm at different velocity. From the left 300RPM, 400RPM, 500RPM and 600RPM

The same behaviour is observable in Fig.5 where the relevant radially averaged axial profile are shown: increasing the impeller velocity, the particle concentration decreases in the lower part of the vessel (where the lower torus is located) and it increases at the quote where the upper torus is placed. Moreover such profiles confirm that almost all particles are essentially attracted by the two tori showing a very low concentration at any agitation speed in the rest of the tank.

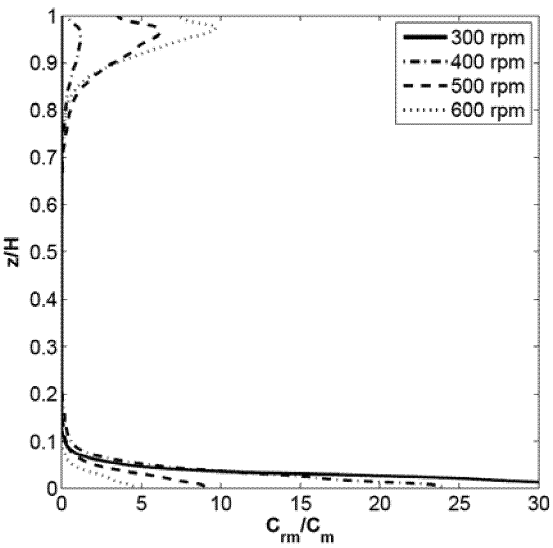

Figure 5: Radially averaged axial profile for glass ballottini of 425-500 μm at different angular velocity

The tori formation has been rarely investigated so far (Abatan et al.,2006). They are likely to result from the complex equilibrium arising among gravity, buoyancy, walls constraining reactions, centrifugal forces, drag

forces and particles inertia. If particles were without their own inertia they would follow the liquid flow field and they would be distributed more or less homogeneously in all the vessel, on the contrary, increasing particles inertia, their tendency to constitute the tori likely increases consequently. In order to better clarify this relationship between particle inertia and tori attraction, the influence of particle diameter and density were investigated.
Figs.6 and 7 show the behaviour of 125-150 μm glass ballottini particles at different angular velocity. It is clear that particles however move preferentially in proximity of the two tori, in fact the particle concentration is higher in the upper and in the lower part of the vessel just where the two tori are placed. But particles with smaller size intrinsically possess a smaller inertia and are more subject to turbulent dispersion forces. This results in a higher homogeneity degree with respect to the case of larger particles.

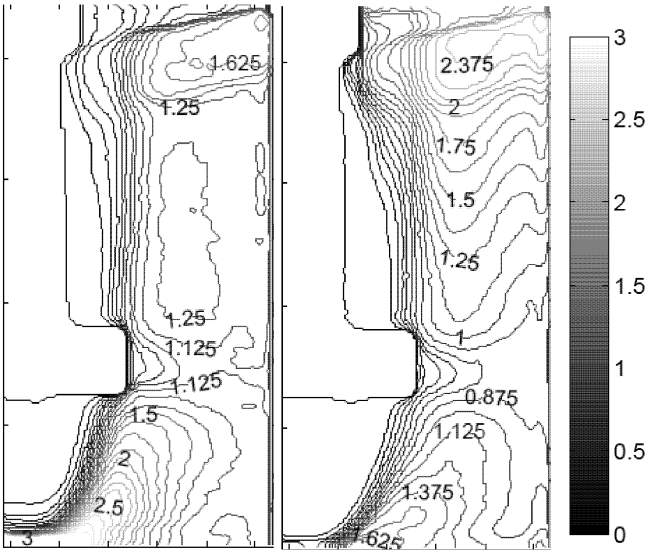

Figure 6: Contour plot of glass ballottini of 125-150 μm at 300RPM (on the left) and 600RPM (on the right)

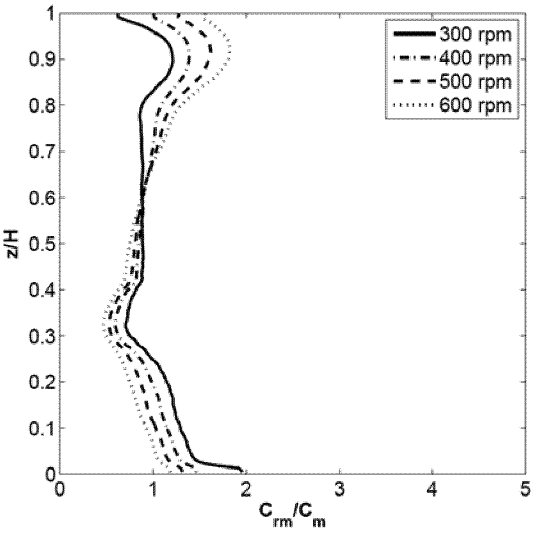

Figure 7: Radially averaged axial profile for glass ballottini of 125-150 μm at different angular velocity

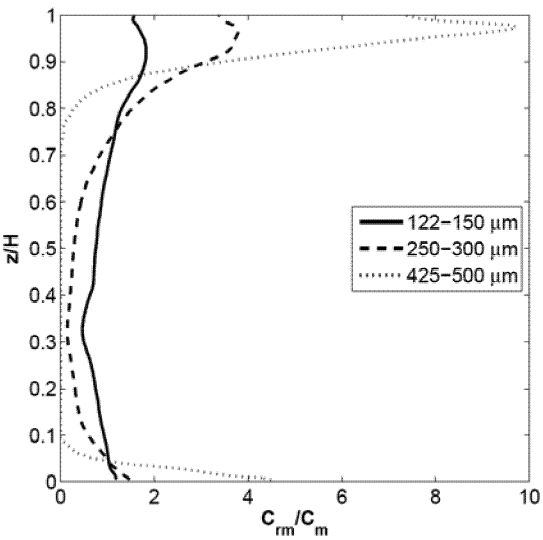

Figure 8: Radially averaged axial profile at 600RPM for glass ballottini of different size

The dependence of particle distribution on particle diameter is better shown in Fig.8 where radially averaged axial profiles relevant to different particle size at constant agitation speed and particle density are shown. Bigger particles are less dispersed and more concentrated in the tori zones because particles with a higher diameter have got a higher inertia.
Also the effect of particle density on the two tori consistency was investigated with results reported in Figs.9 and 10. Increasing particle density at constant agitation speed and particle diameter results in an increase of particle inertia. Even in this case the particle homogeneity degree decreases and the concentration consequently increases near the tori zones.

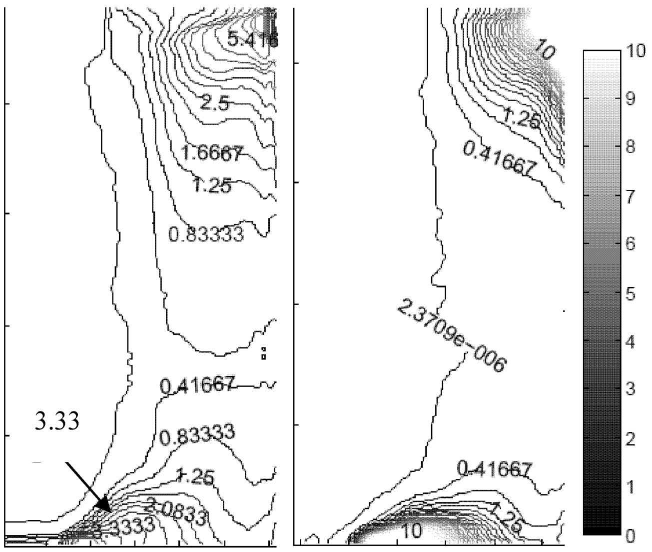

Figure 9: Contour plot at 500 RPM of glass ballottini on the left) and corundum particles (on the right) of 250-300 μm.

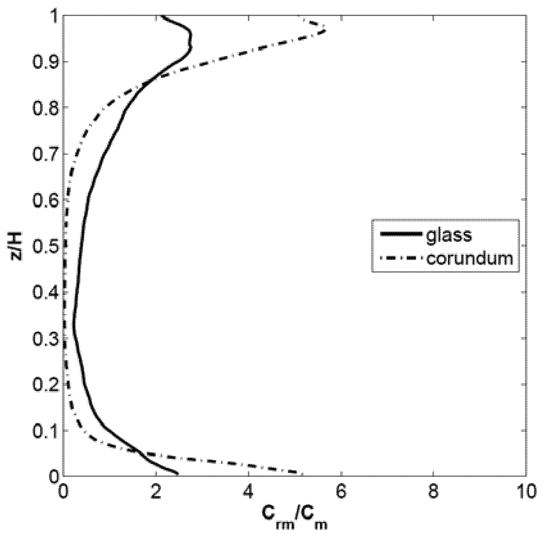

Figure 10: Radially averaged axial profile at 500RPM for glass ballottini and corundum particles of 250-300 μm

Summarizing, particles with a higher inertia have got a higher tendency not to follow the liquid main flow and concentrate in the toroidal attractors, thus resulting in a lower dispersion degree.

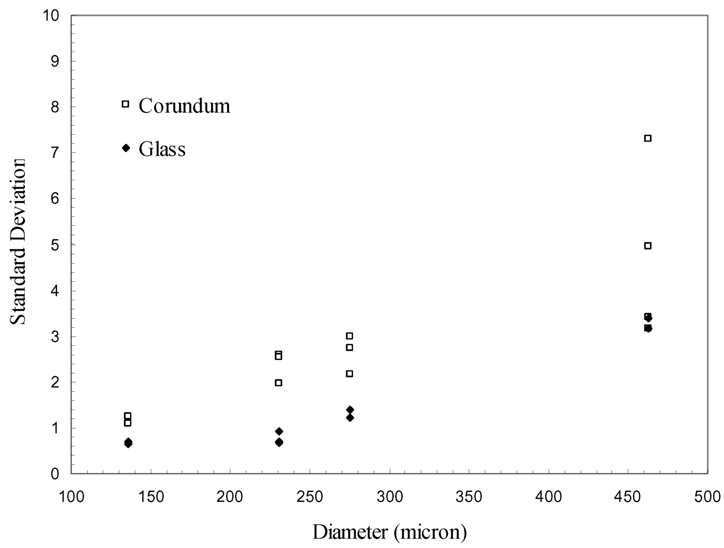

Figure 11: Inertia influence on particle dispersion degree.

The standard deviation of the normalized particle distribution matrixes was also computed and the relevant trend is depicted in Fig.11. In this figure only the results relevant to cases where the agitation speed is higher than the just suspended speed are presented. This is because under incomplete suspension conditions the standard deviation would be heavily affected by the presence of particles resting on the bottom.

4. CONCLUSIONS

A novel technique named *Laser Sheet Image Analysis* was developed and accurately described. It is able to provide directly and in a not invasive way, 2-D solid particles distribution maps in stirred tanks. It was applied to a dilute solid-liquid dispersion in an unbaffled stirred tank provided with a cover at the top.
Visual observation of this unbaffled system show the existence of two stable toroidal attractors for non-Brownian solid particles heavier than the fluid. The existence conditions and possible influences on the formation of these two tori for solid particles were investigated.
LSIA technique appear to be very useful and promising: it was able to reproduce the same system behaviour visually observed. Results show that particle diameter and density affect the attraction of the two tori and the particle suspension degree consequently.
By discussing these results it can be stated that the tori formation, opposing to particle dispersion, is favoured by an increase in particle inertia properties.

5. AKNOWLEDGEMENTS

The authors wish to thank Ing. Leonardo Gentile and Ing. Salvo Noto for their help in performing many of the experiments presented in this work
This work was carried out under financial support by Ministero dell'Università e della Ricerca, PRIN-2006 contract n° 2006091953_004.

6. REFERENCES

Abatan, A.A., McCarthy, J.J., Vargas, W.L., 2006. Particle migration in the rotating flow between co-axial disks. AIChE Journal, 52 (6), 2039-2045.
Alba, F., Crawley, G.M., Fatkin, J., Higgs, D.M.J., Kippax P.G., 1999. Acoustic spectroscopy as a technique for the particle sizing of high concentration colloids, emulsions and suspensions. Colloids and Surfaces A: Physiochemical and Engineering Aspects, 153, 495-502.
Aloi L.E., Cherry, R.S., 1996. Cellular response to agitation characterized by energy dissipation at the impeller tip. Chem.Eng.Sci., 51 (9), 1523-1529.
Angst R., Kraume M., 2006. Experimental investigations of stirred solid/liquid systems in three different scales: Particle distribution and power consumption. Chemical Engineering Science , 61, 2864–2870.
Assirelli, M., Bujalski,W., Eaglesham, A., Nienow, A.W., 2008. Macro- and micromixing studies in an unbaffled vessel agitated by a Rushton turbine. Chem.Eng.Sci., 63, 35-46.
Bamberger, J.A., Greenwood, M. S., 2004. Using ultrasonic attenuation to monitor slurry mixing in real time. Science Direct, 145-148.
Barigou M., Fairhurst P.G., Fryer P.J., Pain J.P., 2003. Concentric flow regime of solid-liquid food suspension: theory and experiment. Chem.Eng.Sci., 58, 1671-1686.
Barresi A. and Baldi G., 1987. Solid dispersion in an agitated vessel. Chemical Engineering Science, 42 (12), 2949-2956.
Bohnet M. and Niesmak G., 1980. Distribution of solids in stirred suspensions. Germ. Chemical Engineering, 3, 57-65.
Brunazzi E., Galletti C., Paglianti A. and Pintus S., 2004. An impedance probe for the measurements of flow characteristics and mixing properties in stirred slurry reactors. Chemical engineering research and design, 82, 1250-1257.
Fangary Y.S., Barigou M., Seville J.P.K. and Parker D.J., 2002. A Lagrangian study of solids suspensions in a stirred vessel by Positron Emission Particle Tracking (PEPT). Chemical Engineering Technology, 25, 521-528.

Fournier, T. and Jeandey, C., 1993, "Optimization of an experimental setup for void fraction determination by the X-ray attenuation technique", in J.M. Delhayr and G. Cognet (Eds.), *"Measuring techniques in gas-liquid two-phase flows"* (pp. 199-228), Berlin, Heidelberg, New York, Tokio: Springer.
Godfrey, J.C. and Zhu, Z.M., 1994. Measurement of particle-liquid profiles in agitated tank. AIChe Symp. Series, 90, 181-185.
Guida, A., Fan, X., Parker, D.J., Nienow, A.W., Barigou, M., 2009. Positron emission particle tracking in a mechanically agitated solid-liquid suspension of coarse particles. Chemical Engineering Research and Design, 87 (4), 421-429.
Hekmat , D., Hebel, D., Schmid, H., Weuster-Botz D., 2007. Crystallization of lysozyme: from vapor diffusion experiments to batch crystallization in agitated ml-scale vessels. Process Biochemistry, 42, 1649-1654.
Lu, WM., Hsu, RC., Chien, WC., Lin, L.C., 1993. Measurement of local bubble diameters and analysis of gas dispersion in an aerated vessel with disk-turbine impeller. Journal of Chemical Engineering Japan, 26, 551-557.
Magelli F., Fajner D., Nocentini M. and Pasquali G., 1990. Solid distribution in vessels stirred with multiple impellers. Chem.Eng.Sci., 45 (3), 615-625.
McKee S.L., Williams R.A. and Boxman A., 1995. Development of solid-liquid mixing models using tomographic techniques. Chemical Engineering Journal, 56, 101-107.
Pacek, A. W., Ding, P., Nienow, A.W., 2001. The effect of volume fraction and impeller speed on the structure and drop size in aqueous/aqueous dispersions. Chem.Eng.Sci., 56, 3247-3255.
Parker, D. J., Broadbent, C. J., Fowles, P., Hawkesworth, M. R., McNeil, P., 1993. Positron emission particle tracking - A technique for studying flow within engineering equipment. Nuclear Instruments and Methods in Physics Research, A326, 592–607.
Rousseaux, J.M., Muhr, H., Plasari, E., 2001. Mixing and micromixing times in the forced vortex region of unbaffled mixing devices. Can.Jour.Chem.Eng. 79, 697–707.
Sessiecq P., Mier P., Gruy F. and Cournil M., 1999. Solid particles concentration profiles in an agitated vessel. Institution of Chemical Engineers, Trans IChemE, 77 (A), 741-746.
Spidla M., Sinevic V., Jahoda M., Machon V., 2005. Solid particle distribution of moderately concentrated suspensions in a pilot plant stirred vessel. Chemical Engineering Journal, 113, 73-82.
Thompson, V.S., Worden, R.M., 1997. Phase hold-up, liquid dispersion, and gas-to-liquid mass transfer measurements in a three-phase magnetofluidized bed. Chemical Engineering Science, 52, 273-295.
Wang M., Dorward A., Vlaev D. and Mann R., 2000. Measurements of gas-liquid mixing in a stirred vessel using electrical resistance tomography (ERT). Chem.Eng.J., 77, 93-98.